

# Fully differential cross sections for photo double ionization of fixed-in-space D<sub>2</sub>

Th. Weber<sup>1,4,6</sup>, A. Czasch<sup>1</sup>, O. Jagutzki<sup>1</sup>, A. Müller<sup>1</sup>, V. Mergel<sup>1</sup>, A. Kheifets<sup>2</sup>, J. Feagin<sup>3</sup>,  
E. Rotenberg<sup>4</sup>, G. Meigs<sup>4</sup>, M.H. Prior<sup>4</sup>, S. Daveau<sup>4</sup>, A.L. Landers<sup>5</sup>, C.L. Cocke<sup>6</sup>,  
T. Osipov<sup>6</sup>, H. Schmidt-Böcking<sup>1</sup> and R. Dörner<sup>1,\*</sup>

<sup>1</sup>*Institut für Kernphysik, Universität Frankfurt, D 60486 Frankfurt, Germany*

<sup>2</sup>*Research School of Physical Sciences and Engineering, Australian National University, Canberra ACT 0200, Australia*

<sup>3</sup>*Dept. of Physics, California State University-Fullerton, Fullerton, CA 92834*

<sup>4</sup>*Lawrence Berkeley National Laboratory, Berkeley CA 94720*

<sup>5</sup>*Dept. of Physics, Western Michigan University, Kalamazoo, MI 49008*

<sup>6</sup>*Dept. of Physics, Kansas State University, Manhattan, KS 66506*

\*Electronic address: [doerner@hsb.uni-frankfurt.de](mailto:doerner@hsb.uni-frankfurt.de)

(August 1, 2003)

PACS: (33.60.Cv), (33.80.Eh), (31.15.Ar)

**Abstract:** We present the first report on the angular distributions of two electrons ejected from a fixed-in-space D<sub>2</sub> molecule by the absorption of a single photon. We focus on equal energy sharing of the two emitted electrons while the photon energy was 75.5 eV. We observed the theoretically predicted relaxation of one of the selection rules valid for He photo double ionization but removed for D<sub>2</sub>. For coplanar geometry of the two-electron escape we found a strong dependence of the electron angular distribution on the orientation of the molecular axis relative to the linear polarization axis of the light. This effect is reproduced qualitatively by a simple theoretical model in which a pair of photo ionization amplitudes is introduced for the light polarization parallel and perpendicular to the molecular axis. These amplitudes are calculated in the single-center approximation.

Simultaneous ejection of two electrons by absorption of a single photon (Photo Double Ionization or PDI) has become a paradigm for studying dynamics of electron-electron correlation. However, until now, only the simplest process of this kind, PDI of helium, is sufficiently well understood (see [1]). A more intricate PDI process is the photo fragmentation of the hydrogen H<sub>2</sub> (or deuterium D<sub>2</sub>) molecule. In this process, the departure of the two photoelectrons is followed by the Coulomb explosion of the two bare nuclei. Here we report on the first kinematically complete photo fragmentation study of the fixed-in-space D<sub>2</sub>.

In the pioneering experiments on PDI of H<sub>2</sub>, the ionic fragments were detected yielding the total cross section and the ion angular distribution ([2], [3]). More recently, electron-electron coincidence ( $\gamma, 2e$ ) experiments without detection of the ions ([4], [5], [6], [7]), and electron-ion coincidences without detection of the second electron [8] became feasible. The ( $\gamma, 2e$ ) experiments revealed surprising similarity between the coincident electron angular distributions for He and D<sub>2</sub>. For He, at the excess energies up to 100 eV above the threshold, these angular distributions (Fully Differential Cross Sections - FDCS) are known to be governed by two major effects: the final state repulsion of the two electrons and selection rules resulting from the <sup>1</sup>P<sup>o</sup> symmetry of the final two-electron state [1]. One might expect that the

influence of the final state repulsion is similar for H<sub>2</sub> and He since the photoelectrons depart quickly compared to a slow motion of the heavy nuclei. Hence, at large distances, the photoelectrons move in the Coulomb field of a point charge  $Z = 2$  for most geometrical configurations. Not surprisingly, a helium-like model introduced by Feagin [9] and later extended by Reddish and Feagin [10] provided a fairly good description of the experimental data of Wightman et al. [5] obtained on randomly oriented D<sub>2</sub> molecules. Feagin [9] introduced two complex symmetrized amplitudes  $g_{\Sigma}$  and  $g_{\Pi}$  which corresponded to the PDI by light polarized along and perpendicular to the molecular axis, respectively. A Gaussian representation of these amplitudes was used as expected from Wannier theory.

Despite this similarity of the PDI of He and H<sub>2</sub> some selection rules which exclude certain escape geometries are relaxed for H<sub>2</sub> ([9], [11]). Primarily, this relaxation of the selection rules stems from the fact that the angular momentum of the photoelectron pair is not a good quantum number; hence the electronic continuum wave function does not have a pure P symmetry. The molecular ground state already has higher angular momentum components and, in addition, electron scattering by the nuclei during ejection from the molecule can lead to angular momentum mixing.

In helium, for equal energy photoelectrons, the cross section is zero on a cone  $\theta_2 = 180^\circ - \theta_1$ , where  $\theta_{1,2}$  are

the polar angles of electrons 1 and 2 with respect to the polarization axis (see selection rule F in fig. 1 and [1]). In the case of the coplanar geometry (electron momenta and the polarization axis of the light lie in the same plane) this selection rule forbids the back-to-back emission. However, parity conservation also forbids equal energy back-to-back emission (selection rule C in fig. 1 and [1]), thus for He these two rules (F and C) doubly forbid this escape configuration. For H<sub>2</sub>, only the back-to-back emission (selection rule C) is forbidden [11] whereas the rest of the cone becomes accessible for most molecular orientations. Until recently, this theoretical prediction has been confirmed indirectly as only the coplanar data integrated over the molecular axis orientation were available. By performing the PDI measurement on the molecule fixed in space we demonstrate that the change of symmetry and the respective relaxation of the  $\theta_2 \neq 180^\circ - \theta_1$  selection rule are clearly visible for out-of-plane geometries and have a very strong influence on the electron angular distribution. In the meantime, an atomic-like description of the PDI of H<sub>2</sub> due to Feagin [9] remains a good approximation even for the fixed-in-space molecule. We were able to reproduce qualitatively our experimental data by calculating amplitudes  $g_{\Sigma}$  and  $g_{\Pi}$  in a simple single center model.

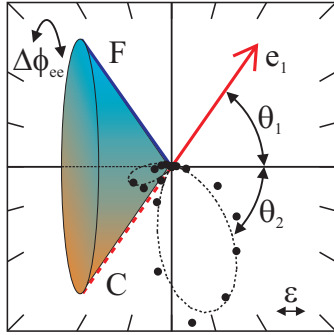


**Figure 1:** Illustration of the selection rules: The dots show the FDSC for the PDI of helium at 24 eV above threshold for equal energy sharing ( $E_1/(E_1+E_2) = 0.5 \pm 0.1$ ). The polarization axis is horizontal. The first electron is fixed at  $\theta_1 = 55^\circ \pm 12^\circ$  as indicated by the (red) arrow. For equal energy sharing the two-electron states with  $^1P^o$  symmetry (e.g. the final state after PDI of He) have a node for  $\theta_2 = 180^\circ - \theta_1$  indicated schematically by the cone (selection rule F), where  $\theta_{1,2}$  are the polar angles of electron 1 and 2 with respect to the polarization axis (see [12]). The dashed straight (red) line indicates the forbidden back-to-back emission (selection rule C). The dashed line represents a Gaussian fit function ( $\Delta\theta_{12} = 99.5^\circ \pm 1.5^\circ$ ).

We have utilized the COLTRIMS technique [13] to measure two electrons and both ionic fragments in a four-fold coincidence experiment. The photon beam from beamline 7.013 of the Advanced Light Source at Lawrence Berkeley National Laboratory, operated in double bunch mode, was intersected with a supersonic

molecular beam of D<sub>2</sub>. The charged particles were guided by electric and magnetic fields onto two position sensitive channel plate detectors capable of registering multiple hits using rectangular and hexagonal delay line anodes (see [14]). We have performed two experiments at the same photon energy but different guiding field and spectrometer configurations. Each of the experiments involved about 8 days of data collection. In both experiments the guiding fields assured  $4\pi$  collection efficiency for all particles. However, a multihit dead time on the electron detector and a vanishing momentum resolution for those electrons performing integer number of revolutions in the solenoidal magnetic field (see [15]) yielded some dead areas in the multidimensional phase space of each of the experiments. The geometry and fields in both experiments were chosen such that the observed regions of phase space complemented each other and the two data sets could be merged into one thus covering the complete final state. One of the experiments used a weak electric field for the electron collection followed by a high pulsed field for the ion collection. Each experiment on D<sub>2</sub> was followed by an experiment on He at the same excess energy using the same spectrometer settings. Since the results for He are well established, these could be used as an independent check of the experimental setup.

The fully differential cross section (FDSC)  $d\sigma^6/d\theta_1 d\theta_2 d\Delta\phi_{ee} d\theta_R d\Delta\phi_{eR} dE_1 dE_2$  depends on the polar angles  $\theta_{1,2,R}$  of electrons 1 and 2 and the internuclear axis R with respect to the polarization axis, on the difference of the azimuthal angles  $\Delta\phi_{ee} = \phi_1 - \phi_2$  of the two electrons as well as the difference between the azimuthal angles of the first electron and the molecular axis  $\Delta\phi_{eR} = \phi_1 - \phi_R$ , and on the energies  $E_1, E_2$  of both electrons. In this definition of angles the coplanar geometry of references ([4], [5], [6] and [7]) corresponds to  $\Delta\phi_{ee} = 0, 180^\circ$ , back-to-back emission of both electrons is  $\Delta\phi_{ee} = 180^\circ$ ,  $\theta_2 = 180^\circ - \theta_1$ .

Figure 2 shows the FDSC for D<sub>2</sub> at different molecular orientations in comparison with analogous data for helium. The helium data (figure 2d) display the well known structure of two lobes separated by the area at  $\theta_2 = 180^\circ - \theta_1$  which is forbidden by the selection rule F. This is indicated by the vertical dashed line which corresponds to the three dimensional cone shown in fig. 1 (see also fig. 11 in Ref. [16] and fig. 2 in Ref. [12]).

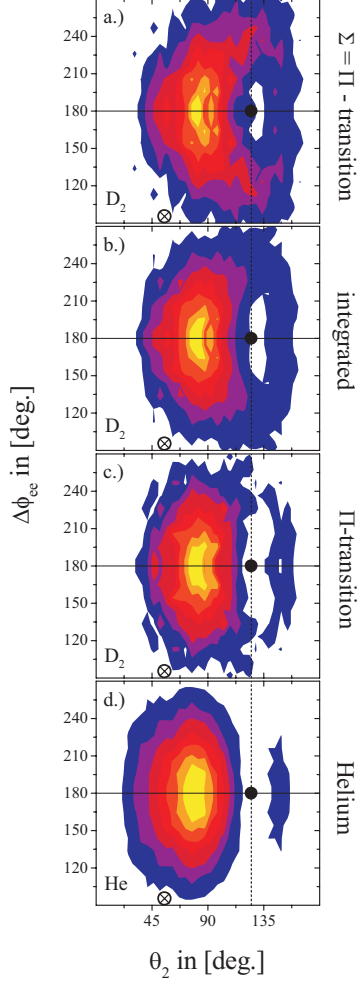


**Figure 2:** A density plot of the angular distribution of the second electron if the first electron is detected at  $\theta_1 = 55^\circ \pm 12^\circ$  as indicated by the circled cross. The patterns show the photo double ionization of  $D_2$  (a-c) at 75.5 eV and He (d) at 103 eV photon energy corresponding to a similar sum electron energy of 24 eV for equal energy sharing ( $E_1/(E_1+E_2) = 0.5 \pm 0.1$ ) and linearly polarized light. Horizontal axis: polar angle  $\theta_2$  of electron 2 with respect to the polarization axis, vertical axis: difference between the azimuthal angles of the two electron  $\Delta\phi_{ee}$ . The back-to-back emission is indicated by the full dot on the  $\Delta\phi_{ee} = 180^\circ$  line. The dashed vertical line represents the nodal cone  $\theta_2 = 180^\circ - \theta_1 = 125^\circ$  as discussed in the text. The color scale is linear in the count rate. (a)  $D_2$  molecule  $\theta_R = 45^\circ \pm 11^\circ$ , i.e. a mixture of  $\Sigma$  and  $\Pi$  transition (integrated over  $\Delta\phi_{eR}$ ), (b)  $D_2$  integrated over all molecular orientations, (c)  $\theta_R = 90^\circ \pm 11^\circ$ , i.e.  $\Pi$  transition (integrated over  $\Delta\phi_{eR}$ ). (d) Helium. For better statistical evidence the data have been mirrored along the  $\Delta\phi_{ee} = 180^\circ$  line.

As predicted by Walter and Briggs (selection rules H and I in [11]), the nodal cone, and hence the He-like FDCS, is also observed for  $D_2$  when the molecular axis is parallel or perpendicular to the polarization of light and only one amplitude  $f_\Sigma$  (not shown here) or  $f_\Pi$  (figure 2c) contributes to PDI. For arbitrary orientation of the

molecule the nodal cone fills up due to interference between the  $f_\Sigma$  and  $f_\Pi$  amplitudes. This interference is weighted by the factor  $\cos\theta_R \cdot \sin\theta_R$  which is strongest at the molecular orientation angle  $\theta_R = 45^\circ$ . Indeed, our  $D_2$  data taken at  $\theta_R = 45^\circ$  show that the forbidden area is reduced to a singular node for back-to-back emission (indicated by the black dot in figure 2a: selection rule C). After integration over all molecular axis orientations (figure 2b) the filling of the node becomes less prominent as compared to the pure  $\theta_R = 45^\circ$  case. This is because of the dominating  $\Pi$  transition (compare with [2]). Note that the maximum for  $D_2$  is slightly shifted to the left as compared to He. This is consistent with the observation made in the coplanar geometry when both photoelectrons and the polarization vector belong to the same plane ([4], [5], [6] and [7]). This corresponds to a slice through figure 2b along the  $\Delta\phi_{ee} = 0^\circ$  and  $\Delta\phi_{ee} = 180^\circ$  line. The authors of references [4], [5], [6] and [7] also observed a slight filling of the node for back-to-back emission. It was argued that an apparent filling of the node was a consequence of a finite experimental acceptance angle in  $\Delta\phi_{ee}$  ([9], [10]). Our data confirm this explanation directly.

We now will concentrate on the coplanar geometry where the photoelectrons, molecular and polarization axes are bound to the same plane which, in our notations, corresponds to  $\Delta\phi_{ee} = 0, 180^\circ$  and  $\Delta\phi_{eR} = 0, 180^\circ$ . Choosing this specific geometry allows us to investigate in more detail the influence of the molecular axis orientation on the photoelectron angular distributions. These distributions are presented in figure 3 for equal energy sharing.

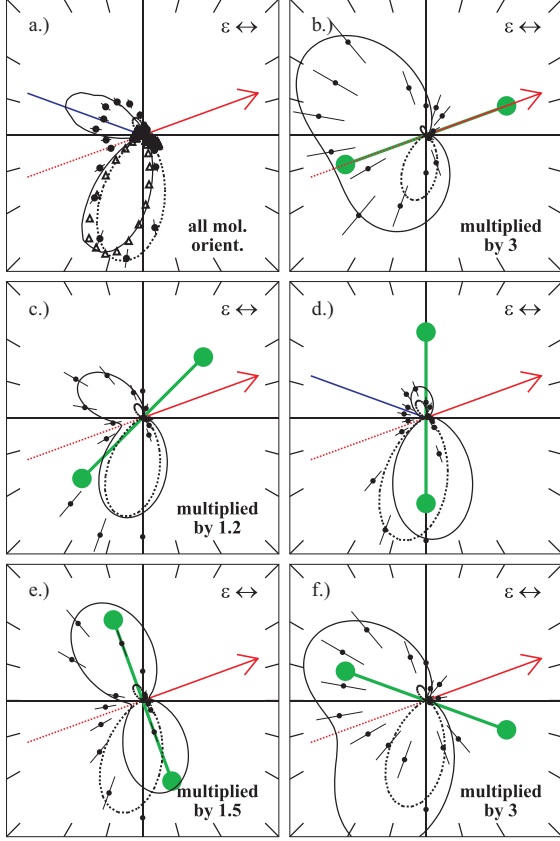


**Figure 3:** FDCS for PDI of  $D_2$ , equal energy sharing  $E_1/(E_1+E_2) = 0.5 \pm 0.1$ ,  $\theta_1 = 20^\circ \pm 10^\circ$  indicated by the (red) arrow, polarization vector horizontal, electron 2 coplanar. Panel (a): integrated over all molecular axis orientations. Panels (b)-(f): molecule coplanar ( $\Delta\phi_{eR} = 0, 180^\circ \pm 45^\circ$ ) and (b)  $\theta_R = 20^\circ$ , (c)  $\theta_R = 45^\circ$ , (d)  $\theta_R = 90^\circ$ , (e)  $\theta_R = 110^\circ$ , (f)  $\theta_R = 160^\circ$  (all  $\pm 12^\circ$ ). The data are internormalized for all angles  $\theta_R$ , an extra multiplier is introduced for better visibility as indicated in each panel. The calculation (solid line) corresponds to Eq. (5) and (6) of Feagin [9] on panels (a) and (b-f), respectively. The open triangles in (a) represent the same calculation in which we set  $f_\Sigma = f_\Pi$ . The dashed lines in all pictures show the Gaussian fit of the helium calibration data of this measurement (according to fig. 1). The dashed straight (red) line indicates selection rule C. The straight solid (blue) line in (a) represents selection rule F valid on a cone in the PDI of helium. In (d) this rule has to be transferred in the body fixed frame as stated in [11].

The data presented on panel (3a) are integrated over all molecular orientations. The solid line on the same panel shows the spherically averaged FDCS calculated using Eq. (6) of Feagin [9]. To evaluate the amplitudes  $f_\Sigma$  and  $f_\Pi$  we employed a simple model in which we used a single-center expansion of the  $H_2$  ground state [17], and a convergent close-coupling (CCC) expansion of the final two-electron state in the field of a point-like charge  $Z = 2$  [18].

For comparison, we present the interference-free FDCS calculated with  $f_\Sigma = f_\Pi$  (shown as the open triangles). As the result of the interference of  $f_\Sigma$  and  $f_\Pi$ , the main lobe

in the spherically averaged FDCS for  $H_2$  is slightly shifted backwards, i.e. here the two electrons repel each other more strongly than in the case of helium. This is also true for the experimental data. The more prominent difference in the data, however, is the increase of the upper lobe. This increase is very strong in the single-center calculation. We see also a filling of the node for back-to-back emission, which is due to our rather large azimuthally acceptance angle in  $\phi_{ee} = 180^\circ \pm 30^\circ$ . A similar effect was observed in [4], [5] and [10].

The difference between  $D_2$  and He, while not strikingly apparent in the averaged data (see figure 3a), is marked when appropriate conditions are chosen. The fixing of the molecular orientation (figure 3b-f) leads to a very strong dependence of the angular distribution on the molecular axis orientation; now different angular distributions can be obtained. Only for a pure  $\Sigma$  (not shown here) and  $\Pi$  transition (panel 3d) is a structure similar to the He case observed. For other molecular orientations, the upper lobe, which is negligible for He, is much stronger or dominates for  $D_2$ . This dramatic change in the angular distributions highlights the subtle interplay of selection rules and electron repulsion which influences the FDCS. As outlined above, the  $\theta_2 \neq 180^\circ - \theta_1$  selection rule (nodal cone in figure 1) holds exactly for He and for the pure  $\Sigma$  or  $\Pi$  transition in  $D_2$ . This nodal cone leads to nodes along the dashed (red) and straight (blue) line in figure 3d ( $\Pi$  transition). However, for molecular orientations other than  $0^\circ$  and  $90^\circ$ , only the singular nodal point of the back-to-back emission [selection rule C, straight dashed (red) line] survives and the node in the upper half plane vanishes. As a consequence a significant electron flux is observed in the upper half plane. This contribution results from the interference of the  $g_\Pi$  and  $g_\Sigma$  amplitudes.

The solid line on the same panels (3b-f) shows the calculated FDCS obtained by feeding the single-center amplitudes into Eq. (5) of Feagin [9]. Due to a very strong dependence of the FDCS on the molecular orientation we had to convolute our calculation with a finite acceptance angles and energy sharing ratio. The calculation reproduces the main features of the experiment. Not only the shape but also the cross section changes strongly with the molecular axis rotation (see scaling factors and caption in figure 3). The contribution of  $g_\Pi$  is much weaker than  $g_\Sigma$  for intermediate angles  $\theta_R$ .

It is noteworthy that a Gaussian parametrization applies well to both amplitudes  $g_\Pi$  and  $g_\Sigma$  giving their magnitude ratio  $g_\Pi/g_\Sigma = -1.1$  and their FWHM  $\Delta\theta_{12}^\Sigma = 70.0^\circ$  and  $\Delta\theta_{12}^\Pi = 78.8^\circ$ . This is to be compared with the Gaussian parameters  $g_\Pi/g_\Sigma = -2.2$  and  $\Delta\theta_{12}^\Sigma = \Delta\theta_{12}^\Pi = 76 \pm 3^\circ$  reported by Feagin [9] who fitted spherically averaged FDCS. If a similar fitting procedure was applied to the present fixed-in-space FDCS (not shown

here), the same magnitude ratio is obtained but the width parameters are different:  $\text{FWHM } \Delta\theta_{12}^{\Sigma} = 83.5^{\circ}$  and  $\Delta\theta_{12}^{\Pi} = 61.5^{\circ}$ .

In summary, we have observed significant variation of the FDCS between He and D<sub>2</sub> for the non coplanar geometry and for mixed  $\Sigma$  and  $\Pi$  transitions, i.e. for the molecular axis neither parallel nor perpendicular to the polarization. The coplanar geometry data are well reproduced by the He-like theory of Feagin [9] with a pair of fixed polarization amplitudes  $g_{\Sigma}$  and  $g_{\Pi}$ . Interference of these amplitudes leads to a strong dependence of the FDCS on the molecular axis orientation. We calculate the amplitudes by applying the single-center expansions both to the molecular ground state and the final two-electron state. The similarity between the theoretical and experimental FDCS indicates the degree to which the angular correlation pattern is formed mainly by the electron-electron correlation in the final state at fairly large distances from the molecular ion. The non-zero angular momentum components of the H<sub>2</sub> ground state also play a role. A pure S-symmetry ground state would result in the magnitude ratio  $g_{\Sigma}/g_{\Pi} = -1$ . Experimental data show strong deviation from this ratio, stronger than can be produced by a single-center model. This indicates that a proper molecular calculation might result in a better agreement with the experiment.

#### Acknowledgements

This work was supported in part by DFG, BMBF, Chemical Sciences, Geosciences and Biosciences Division, Office of Basic Energy Sciences, Office of Science, U.S. Department of Energy (DOE). The Advanced Light Source is supported by the DOE under Contract No. DE-AC03-76SF00098. Th. W. thanks Graduiertenförderung des Landes Hessen, the Alexander von Humboldt Stiftung and the Herrmann Willkomm Stiftung for financial support. We thank Roentdek GmbH (www.Roentdek.com) for support with the delay line

detectors. We acknowledge very helpful discussion with our colleagues M. Walter, J. Briggs, T. Reddish and V. Schmidt.

#### References

- [1] J. Briggs and V. Schmidt, *J. Phys. B*, **33**, (2000), R1
- [2] H. Kossmann et al., *Phys. Rev. Lett.*, **63**, (1989), p. 2040
- [3] G. Dujardin, *Phys. Rev. Lett.*, **35**, (1987), p. 5012
- [4] T. Reddish et al., *Phys. Rev. Lett.*, **79**, (1997), p. 2438
- [5] J. Wightman, S. Cvejanovic and T. Reddish, *J. Phys. B*, **31**, (1998), p. 1753
- [6] S.A. Collins et al., *Phys. Rev. A*, **64**, (2001), p. 2706
- [7] D.P. Seecombe et al., *J. Phys. B*, **35**, (2002), p. 3767
- [8] R. Dörner et al., *Phys. Rev. Lett.*, **81**, (1998), p. 5776
- [9] J.M. Feagin, *J. Phys. B*, **31**, (1998), L729
- [10] T.J. Reddish and J.M. Feagin, *J. Phys. B*, **32**, (1999), p. 2473
- [11] M. Walter and J.S. Briggs, *Phys. Rev. Lett.*, **85**, (2000), p. 1630
- [12] F. Maulbetsch and J. Briggs, *J. Phys. B*, **28**, (1995), p. 551
- [13] R. Dörner et al., *Physics Reports*, **330**, (2000), p. 96
- [14] O. Jagutzki et al., *IEEE Trans. Nuc. Sci.*, **49**, (2002), p. 2477
- [15] R. Moshhammer et al., *Nucl. Instr. Meth. B*, **107**, (1996), p. 62
- [16] Dörner et al., *Phys. Rev. A*, **57**, (1998), p. 1074
- [17] H.W. Joy and R.G. Parr, *J. Comp. Phys.*, **28**, (1958), p. 448
- [18] A.S. Kheifets and I. Bray, *J. Phys. B*, **32**, (1998), L447